Available online at www.sciencedirect.com

ScienceDirect

Physics Procedia (2015) 000–000

Physics
Procedia

www.elsevier.com/locate/procedia

2015 International Congress on Ultrasonics, 2015 ICU Metz

Analysis of transient acoustic radiation field from pulse-driven finite aperture piezoelectric transducer

Akira Yamada[a]* and Yoshio Udagawa[b]

[a]*Tokyo University of Agriculturee & Tech, 2-24-16,Nakacho, 184-8588 Koganei, Tokyo, Japan*
[b]*Imaging Supersonic Laboratories, 12-7 Tezukayama-nakamachi, 631-0063 Nara, Japan*

Abstract

A method is presented for the precise analysis of the discontinuous transient radiation field from a circular piezoelectric transducer in the liquid medium. The transducer is excited by the step pulse voltage signal, on the contrary to the conventional burst sine pulse signals. Specifically, time domain Rayleigh integral formula is extended to include the medium attenuation to meet the actual phenomena in the far field region. As a results, some peculiar characteristics intrinsic to the transient pulse radiation fields are elucidated. Simulation results are also compared with experiments to verify the validity of the proposed methods.

Keywords: Sound wave radiation field; Piezoelectric transducer; Transient propagation; Impulse response; Rayleigh integral analysis

---

1. Introduction

Previous works for the radiation field analysis from finite aperture transducer has been mainly employed for sine continuous or sine burst pulse excitation conditions [1], [2]. Many of the devices, however, are driven by the step or spike pulse signals. If the conventional numerical methods [3] are employed for such excitation conditions, they are hampered by the accumulation of numerical dispersion errors caused by the discontinuous edges of the excitation

---

* Corresponding author. Tel.: +81-42-388-7135; fax: +81-42-388-7442.
E-mail address: yamada@cc.tuat.ac.jp

signals. On this account, behaviors of radiation fields, driven by such discontinuous signals, have never been reported before except for the studies by the present authors [4],[5],[6]. In this paper, a method are presented for the analysis of the transient pulse radiation fields excited by a circular transducer emitted into a homogeneous liquid medium. Specifically, time domain analytical Rayleigh integral formula is extended to include the medium attenuation to meet the actual phenomena in the far field region. As a results, peculiar characteristics intrinsic to the transient radiation fields are elucidated. Simulation results are also compared with experiments to verify the validity of the proposed methods.

2. Radiation sound wave field analysis based on the Rayleigh integral formula

2.1. Basic formulation

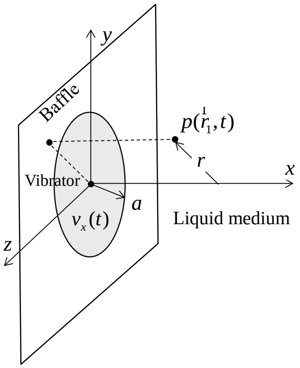

Fig.1. Coordinate assignment in the Rayleigh integral analysis.

A piezoelectric vibrator plate is placed on a rigid baffle with the coordinate assignment as shown in Fig.1. Sound waves are emitted toward a semi-infinite homogeneous liquid medium $x>0$. Uniform piston movement on the vibrator surface, with x-component particle velocity $v_x(t)$ as a function of time t, is assumed. According to the Rayleigh integral formula [1],[2], pressure $p(\vec{r}_1,t)$ at time t and location $\vec{r}_1$ in the right half-plane medium is expressed by

$$p(\vec{r}_1,t)=\rho v_x(t)*\frac{\partial h_0(\vec{r}_1,t)}{\partial t}, \tag{1}$$

where ρ is the mass density of the medium, symbol * denotes the convolution calculation with respect to time t and h_0 is the spatial impulse response between the observation point and the transducer aperture surface. Impulse response h_0 for a circular vibrator with radius a results in a simple analytical formula [1]. It is omitted here because of space limitations.

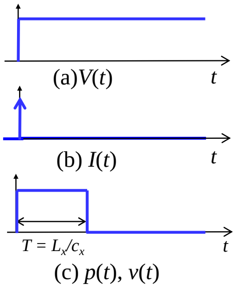
(a)$V(t)$
(b) $I(t)$

(c) $p(t)$, $v(t)$

Fig.2 Excitation waveform.

2.2. Rectangular particle velocity excitation waveform by the step voltage input

As a transient excitation, step voltage V as shown in Fig.2 (a) is applied between the vibrator electrodes. Instantaneous impulse current I as shown in Fig.2 (b) then flows. Caused by the impulse current, constant stress field is induced over the entire vibrator medium instantaneously. Note that the fields in the vibrator are changed only in thickness x-direction. The spatial derivative of the stress field excites the forward and backward propagating waves. Only the forward wave propagates when the rear surface is backed with a highly absorbing material. Let a, L_x and c_x be radius, thickness, and longitudinal sound wave speed of the circular vibrator plate, respectively. Resultant excitation waveform for particle velocity v_x at front surface of the vibrator becomes an unipolar rectangle pulse with duration $T=L_x/c_x$ as shown Fig.2 (c) which is given by,

$$v_x(t,x=0)=v_0\mathrm{rect}(t/T), \tag{2}$$

where v_0 is amplitude of particle velocity and rect() denotes the rectangular function starting at t=0 with unit amplitude and unit duration.

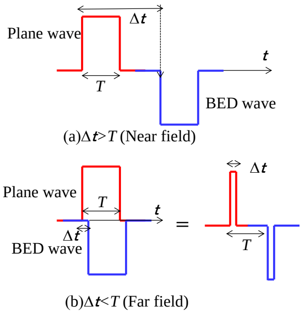

(a)Δt>T (Near field)

(b)Δt<T (Far field)

Fig.3 Schematic of pressure field along the center axis of the vibrator.

2.3. Overview of radiation wave field

As a simple case, we consider the radiation fields on the center axis of the circular plate. Imposing transversal distance $r(=\sqrt{y^2+z^2})$ to be r=0, impulse response h_0 becomes a unipolar rectangular function. That is,

$$h_0(t,x,r=0) = c\,\mathrm{rect}((t-x/c)/\Delta t) = \begin{cases} c, & \text{for } x/c < t < \sqrt{x^2+a^2}/c \\ 0, & \text{elsewhere,} \end{cases} \tag{3}$$

where c is the sound speed of longitudinal wave in the medium and Δt is a time of flight difference between the plane wave and BED wave, which is given by

$$\Delta t = (\sqrt{x^2+a^2} - x)/c\,. \tag{4}$$

Substitution of eq.(2) and time derivative of eq.(3) into eq.(1), axial pressure filed p is obtained as,

$$p(t,x,r=0) = \rho c v_0 \left\{\mathrm{rect}[(t-x/c)/T] - \mathrm{rect}[(t-c/x-\Delta t)/T]\right\}. \tag{5}$$

First term in the right-hand side of eq.(5) represents the planar primary wave. On the other hand, second term represents the BED (Beam Edge Diffusion) wave emitted from the circular border of the plate. From eq.(5), behavior of the axial pressure fields are reviewed as follows. Before that, we define a near field limiting distance x_0 ($=a^2/2cT-cT/2$) as a one where the condition $T=\Delta t$ is satisfied. In the near filed region where the condition $\Delta t>T$ ($x<x_0$) is satisfied, two rectangular waves (plane wave and BED wave) with opposite signs and pulse width T propagates separately as shown in Fig.3 (a). On the other hand, in the far filed region at $\Delta t<T$ ($x>x_0$), two waves get close and overlaps each other with opposite signs. Consequently, they are merged to a bipolar rectangular wave, the pulse width is in inverse proportion to the distance as shown in Fig.3 (b). Fields in the off axis region at inner side (sunny side) of the transducer are similarly described as a superposition of two waves described above. Where the polarity of BED is negative but with much complex function. At the outer side (shadow side) of the transducer, only BED wave with positive polarity propagates, rapidly attenuating their amplitude with increasing distance from the border of the transducer.

2.4. Incorporation of attenuation factor

In the present rectangular pressure wave excitation as described above, the rectangular top amplitude stays almost constant in return for the narrower pulse width. As a result, the bipolar impulse wave is propagated to anywhere if there is no attenuation in the medium. Moreover, it shows constant flat amplitude along transverse direction inside the transducer, and rapidly decrease with departing from the border of the transducer. It is not consistent with the actual experiment. To match the theory, attenuation impulse response $h_a(t)$ is included as follows:

$$h_a(\vec{r}_1,t) = \begin{cases} \dfrac{1}{\alpha|\vec{r}_1-\vec{r}_2|/c}\exp\left[-(t-\dfrac{|\vec{r}_1-\vec{r}_2|}{c})/\alpha\dfrac{|\vec{r}_1-\vec{r}_2|}{c}\right] & for \quad t>\dfrac{|\vec{r}_1-\vec{r}_2|}{c} \\ 0 & elsewhere \end{cases} \tag{6}$$

where $\vec{r}_2$ is the position on the transducer surface, α is the attenuation factor in the medium. Resultant impulse response $h(t)$ with attenuation is calculated from the convolution of $h_0(t)$ and $h_a(t)$ as $h(t)= h_0(t)* h_a(t)$.

3. Test examination

3.1. Experimental method

A circular disk piezoelectric transducer (KGK: B1C20I) with a radius a=10mm and center frequency f_0=1MHz was prepared. It was backed with absorbing material at rear surface and attached with 1/4 λ thickness matching layer at the front surface. Step pulse voltage (300V) was applied by a high switching speed pulser (ISL: BLP4x). It was attached to the side wall of the water tank (400mm x 400mm x 400mm) and sound waves were emitted into the water medium. A receiver transducer (f_0=20MHz, a=1.5mm) was mounted on a XY mechanical stage and scanned in the target region. The receiver transducer was connected to an oscilloscope through the 10:1 high impedance probe. Note that input impedance of the receiver circuit should be high enough to prevent the signal distortion due to the removal of low frequency components.

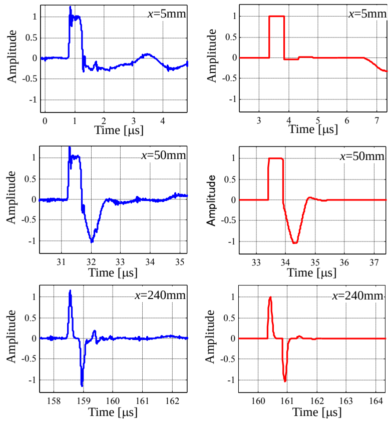

(a)Experiment (b)Simulation

Fig.4 Received wave signals along y=0 center axis at different range positions (x=5, 50, 240mm).

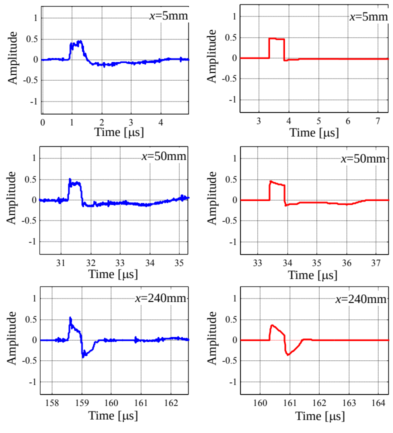

(a)Experiment (b)Simulation

Fig.5 Received wave signals along y=10mm plate border axis at different range positions.

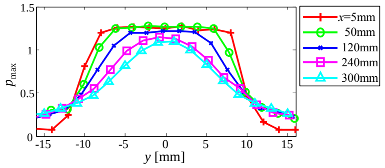

(a)Experiment

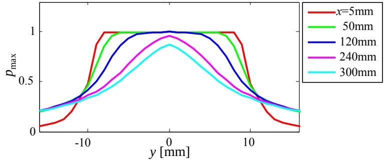

(b)Simulation

Fig.6 Positive peak amplitude profile of received signal along transversal direction: (a) experiment, (b) simulation with attenuation constant α=0.02[Np/μs].

3.2. Results of radiation field measurement

The transient pulse radiation fields were measured over the z=0 horizontal plane ranging x=0-300mm, and y=0-20mm. Experimented received signals along center axis (y=0mm) and plate border (y=10mm) are shown in Fig.4 (a) and Fig.5 (a), respectively. Where results were shown for different range positions at x=5mm, 50mm, and 240mm. Waves were simulated using the present method. Some additional effects in the propagation through matching layer and reflection at backing surface were included, as well as the finite aperture of the receiver transducer. The results were presented as shown in Fig.4 (b) and Fig.5 (b). We can recognize that the experiment results are in good agreement with the theoretical predictions. Finally, positive peak amplitude profiles of received signal along transversal direction are shown in Fig.6. By including attenuation factor (α=0.02[Np/μs]), the results are obtained showing much better agreement between simulation and experiment.

4. Conclusion

Validity of the present Rayleigh integral impulse response approach including attenuation was verified through the comparison between theory and experiment. It was demonstrated that behaviours of transient pulse-driven radiation field were quite different from the conventional sine pulse excitation field. The results may serve for the re-examination of the transducer and device design in NDT and medical applications

References

[1] Stepanishen,P.R., 1971. Transient radiation from pistons in an infinite planar baffle. J.Acoust.Soc.Am.49, 1629-1638.

[2] Jensen,J.A. and Svendsen,N.B.,1992. Calculation of pressure fields from arbitrarily shaped, apodized, and excited ultrasound transducers.IEEE Trans. Ultrason. Ferroelectr. Freq. Control.39, 262-263.

[3] Schechter,R.S., Chaskelis,H.H., Mignogna,R.B., Delsanto,P.P., 1994. Real-time parallel computation and visualization of ultrasonic pulses in solids. Science 265, 1188-92.

[4] Udagawa,Y., 2010. Introduction to Ultrasonic Wave Technique - Transducer, Pulser, Receiver and Device-. Nikkan Kogyo Shimbun, Tokyo.

[5] Yamada,A., Udagawa,Y., 2013. Analysis and observation of sound wave field from finite aperture piezoelectric transducer. Proc. Symp. Ultrasonic Electronics 34, 11-12.

[6] Yamada,A., Udagawa,Y., 2014. Analysis of spatio-temporal radiated acoustic field from finite aperture transducer - Comparison of FDTD numerical computations and Rayleigh integral method -", Proc. Symp. Ultrasonic Electronics 35, 179-180.